J|A|C|S ARTICLES

Published on Web 06/16/2010

Ultrathin Bi_2S_3 Nanowires: Surface and Core Structure at the Cluster-Nanocrystal Transition

Jordan W. Thomson,[†] Ludovico Cademartiri,[‡] Mark MacDonald,[§] Srebri Petrov,[†] Gianluca Calestani,[||] Peng Zhang,[§] and Geoffrey A. Ozin*,[†]

Department of Chemistry, University of Toronto, 80 St. George Street, Toronto, ON, Canada, Department of Chemistry and Chemical Biology, Harvard University, 12 Oxford Street, Cambridge, Massachusetts, Department of Chemistry, Dalhousie University, Halifax, NS, Canada, and Dipartimento di Chimica GIAF, Universita' di Parma, viale Usberti 17, Parma, Italy

Received March 6, 2010; E-mail: gozin@chem.utoronto.ca

Abstract: Herein, we present the structural characterization of the core and surface of colloidally stable ultrathin bismuth sulfide (Bi_2S_3) nanowires using X-ray Absorption Spectroscopy (EXAFS and XANES), X-ray Photoelectron Spectroscopy (XPS), and Nuclear Magnetic Resonance (NMR). These three techniques allowed the conclusive structural characterization of the inorganic core as well as the coordination chemistry of the surface ligands of these structures, despite the absence of significant translational periodicity dictated by their ultrathin diameter (1.6 nm) and their polycrystallinity. The atomic structure of the inorganic core is analogous to bulk bismuthinite, but Bi atoms display a remarkably higher coordination number than in the bulk. This can be only explained by a model in which each bismuth atom at the surface (or in close proximity to it) is bound to at least one ligand at any time.

Introduction

The determination of the structure of nanoscale chemical architectures is one of the long-standing challenges of chemistry and physics. From a structural point of view, most nanostructures are defined by a dense core and a surface. The atomic structure of the core is, depending on the overall dimensions of the nanostructure, either (i) a subset of the corresponding bulk lattice (nanocrystal regime) and still subject to the same translational symmetry operators or (ii) a completely different arrangement of atoms (cluster regime) generally defined by a point symmetry. The cluster to nanocrystal transition usually occurs when the minimum dimension of the nanostructure is approximately 1−2 nm, depending on the electronic properties of the substance. The structure of the surface is reconstructed from the one of the core due to the presence of coordinating ligands, solvation, and high curvature.

The challenges in the determination of surface and core structure originate from limitations in the techniques that are most commonly used. X-ray Diffraction (XRD) relies on coherence lengths of several nanometers, which are often smaller than the characteristic dimensions of the nanostructures being analyzed. In the case of randomly oriented small crystallites (∼1−2 nm), the resulting peak broadening can effectively prevent the unequivocal determination of their structure.[1] Transmission Electron Microscopy (TEM), while having a much shorter coherence length, can only analyze finite numbers of structures, is very time intensive, and is difficult to use on very small structures, due to (i) the lack of image contrast they provide and (ii) their sensitivity to beam damage or beam-induced melting.[2] The structural determination of the surface of nanocrystals by scanning probe techniques is complicated by tight curvatures, and by the presence of organic ligands, which are often coordinating their surface. While these problems prevent in most cases an atom-resolved structural determination, important information on the outer structure of the ligand shell can still be obtained.[3] These challenges can be mostly overcome by the use of XRD on single crystals of nanostructures (supercrystals). This has so far been achieved with gold clusters, but never with nanocrystals.[4] The difficulty in employing this technique arises mostly from the current unavailability of monodisperse nanocrystal dispersions from which such supercrystals can be crystallized. All these techniques are also performed on dry materials, thus preventing them from addressing the structural effects of solvation or ligand exchange.

The structural characterization of structures lying at the cluster-to-nanocrystal transition, where the size of the structure is comparable to the size of the bulk lattice unit cell, is remarkably complex. In this size regime, most of the above-mentioned structural characterization techniques are either underperforming or unsuitable. A spectrum of complementary structural characterization techniques is then necessary to converge reliably on a model of the structure of the core and of the surface.

Our laboratory's recent work on dispersions of colloidal bismuth sulfide (Bi_2S_3) has focused on size and shape control

[†] University of Toronto.
[‡] Harvard University.
[§] Dalhousie University.
[||] Universita' di Parma.

(1) Murray, C. B.; Norris, D. J.; Bawendi, M. G. *J. Am. Chem. Soc.* **1993**, *115* (19), 8706–8715.
(2) Cademartiri, L.; Ozin, G. A. *Adv. Mater.* **2009**, *21*, 1013–1020.
(3) Jackson, A. M.; Hu, Y.; Silva, J.; Stellaci, F. *J. Am. Chem. Soc.* **2006**, *128*, 11135–11149.
(4) Jadzinsky, P. D.; Calero, G.; Ackerson, C. J.; Bushnell, D. A.; Kornberg, R. D. *Science* **2007**, *318*, 430–433.

10.1021/ja101908k

of nanocrystals, nanorods, and ultrathin nanowires.[5,6] The ultrathin nanowires are of particular interest to our group as they have an extremely small diameter (1.6 nm) that places them at the transition between clusters and nanocrystals. Our previous characterization by Powder XRD (PXRD) and TEM provided structural information, but only enough to state that the ultrathin nanowires were likely made of polycrystalline Bi_2S_3 and to propose a preliminary structural model. In fact, HRTEM images of the ultrathin nanowires have proven exceptionally challenging to acquire due to the liquifaction of the nanowires under the electron beam at high magnifications, even at cryogenic temperatures (77 K).

We decided to use three complementary techniques to aquire a deeper understanding of the structure of the inorganic core and coordination chemistry of the surface ligands of ultrathin Bi_2S_3 nanowires: X-ray Absorption Spectroscopy (XAS) including Extended X-ray Absorption Fine Structure (EXAFS) and X-ray Absorption Near Edge Structure (XANES), X-ray Photoelectron Spectroscopy (XPS), and Nuclear Magnetic Resonance (NMR) spectroscopy. Our choice of techniques was predicated upon them being nondestructive to the nanowires, but still able to provide reproducible and quantitative measurements on bond lengths and coordination numbers as well as knowledge concerning the coordination and exchange of capping oleylamine ligands.

EXAFS is especially attractive as (i) it can be performed in the solution phase, (ii) it does not require long-range order, and (iii) it can provide quantitative data on bond lengths and coordination numbers.[7] EXAFS has been used for nanocrystal systems before, with notable examples including an *in situ* study of the structure of colloidal CdSe nanocrystals in *N*,*N*-dimethylformamide (DMF), the observation of both surface Cd−S thiolate bonding and nanocrystal core Cd−Te bonding in thiol capped CdTe nanocrystals, and the study of Au/Pd alloy ultrathin nanowires.[8−10] XANES has also been shown to provide information on structure and electronic properties based on both the characteristic energy of absorption of X-rays by core electrons and the shape of this absorption edge.[11] The characteristic binding energy of core electrons can be measured by XPS and has also been applied to nanocrystals to identify surface species and oxidation states.[12] This technique is far more common as it does not require synchrotron radiation as in the case of XANES and EXAFS.

While these X-ray spectroscopic techniques can provide structural and bonding information about the inorganic core of the nanowires, solution phase Nuclear Magnetic Resonance (NMR) was used to probe the surface properties of the nanowires from the ligand perspective. NMR has long been used as a method to characterize organic molecules and macromolecules and more recently has been applied to the identification of nanocrystal capping ligands, their interaction with the surface of nanocrystals, and their exchange with other ligands.[13−16] In the case of the ultrathin Bi_2S_3 nanowires, the surface makes up more than half of the total atom composition and is thus expected to be important in determining the overall structure and properties of the nanowires. To complement the room temperature solution phase NMR, we also performed Variable Temperature (VT) NMR to probe the dynamic ligand exchange process.[17−19]

The results of this extensive characterization are internally coherent. The atomic structure of the core is consistent with bismuthinite, but with one remarkable difference. The average coordination number of the bismuth atoms is considerably higher than in the bulk. Our results demonstrate that this increased coordination can be attributed to a remarkably dense coordination of the surface bismuth atoms by the capping oleylamine molecules. More specifically, each bismuth atom at the surface (or in proximity of the surface) is capped by *at least* one oleylamine molecule at any one time. NMR characterization demonstrates that, while the density of the capping would suggest that a strong bond is formed between the amine and the surface bismuths, the bond is exclusively dative and the exchange between free and bound ligand occurs faster than ever observed in colloidal nanocrystals. These results further demonstrate how a combination of XAS, XPS, and NMR techniques can allow the structural determination of nanostructures too small for XRD and TEM and too large for Mass Spectrometry (MS).

Experimental Section

Chemicals. Oleylamine (technical grade, 70%), bismuth citrate, sulfur, hexadecylamine (99%), $CDCl_3$, d^8-toluene, and bismuth sulfide (99%) were purchased from Aldrich and used as received. Solvents were from a variety of sources and used as received.

Synthesis of Bi_2S_3 Nanowires. The synthesis of Bi_2S_3 nanowires has been reported elsewhere and can be easily scaled up.[3] Briefly, 3.17 mmol of bismuth citrate were suspended in 4.2 mL of oleylamine in a three-necked flask. The mixture was heated to 100 °C under vacuum and held at this temperature for 30 min. At this point, the flask was put under N_2 and the temperature was increased to 160 °C and held there for 30 min. After this, the temperature was decreased to 130 °C and a solution of 15.6 mmol of sulfur in 10.4 mL of oleylamine was injected in the reaction mixture through a septum. The temperature was increased to 100 °C, and the nanocrystals were grown for between 15 and 45 min. The reaction was quenched with toluene. The product was precipitated with acetone and then centrifuged. The supernatant was removed, and the nanowires were redispersed in toluene. The precipitation/redispersion process was performed twice overall. After purification, care was taken to remove the majority of acetone. For the preparation of NMR samples, the solvent was removed *in vacuo* and dried overnight, and the resulting solid was dispersed in $CDCl_3$

(5) Malakooti, R.; Cademartiri, L.; Akcakir, Y.; Petrov, S.; Migliori, A.; Ozin, G. A. *Adv. Mater.* **2006**, *18*, 2189–2194.
(6) Cademartiri, L.; Malakooti, R.; O'Brien, P. G.; Migliori, A.; Petrov, S.; Kherani, N. P.; Ozin, G. A. *Angew. Chem., Int. Ed.* **2008**, *47*, 3814–3817.
(7) Lee, P. A.; Citrin, P. H.; Eisenberger, P.; Kincaid, B. M. *Rev. Mod. Phys.* **1981**, *53*, 769–806.
(8) Hosokawa, H.; Fujiwara, H.; Murakoshi, K.; Wada, Y.; Yanagida, S.; Satoh, M. *J. Phys. Chem.* **1996**, *100*, 6649–6656.
(9) Rockenberger, J.; Tröger, L.; Rogach, A. L.; Tischer, M.; Grundmann, M.; Eychmüller, A.; Weller, H. *J. Chem. Phys.* **1998**, *108*, 7807–7816.
(10) Teng, X.; Wang, Q.; Liu, P.; Han, W.; Frenkel, A. I.; Wen, W.; Marinkovic, N.; Hanson, J. C.; Rodriguez, J. A. *J. Am. Chem. Soc.* **2008**, *130*, 1093–1101.
(11) Hamad, K. S.; Roth, R.; Rockenberger, T. J.; van Buuren, T.; Alivisatos, A. P. *Phys. Rev. Lett.* **1999**, *83*, 3474–3477.
(12) Katari, J. E. B.; Colvin, V. L.; Alivisatos, A. P. *J. Phys. Chem.* **1994**, *98*, 4109–4117.
(13) Hens, Z.; Moreels, I.; Martins, J. C. *ChemPhysChem* **2005**, *6*, 2578–2584.
(14) Berrettini, M. G.; Braun, G.; Hu, J. G.; Strouse, G. F. *J. Am. Chem. Soc.* **2004**, *126*, 7063–7070.
(15) Owen, J. S.; Park, J.; Trudeau, P.-E.; Alivisatos, A. P. *J. Am. Chem. Soc.* **2008**, *130*, 12279–12281.
(16) Shen, L.; Soong, R.; Wang, M.; Lee, A.; Scholes, G. D.; Macdonald, P. M.; Winnik, M. A. *J. Phys. Chem. B* **2008**, *112*, 1626–1633.
(17) Badia, A.; Cuccia, L.; Demers, L.; Morin, F.; Lennox, R. B. *J. Am. Chem. Soc.* **1997**, *119*, 2682–2692.
(18) Schmid, G. *Struct. Bonding (Berlin)* **1985**, *62*, 51–85.
(19) Petroski, J.; Chou, M. H.; Creutz, C. *Inorg. Chem.* **2004**, *43*, 1597–1599.

or d^8-toluene. Samples were centrifuged to remove insoluble material. The resulting concentrations were approximately 20 mg/mL.

Ligand Exchange with Hexadecylamine. A large excess of hexadecylamine in chloroform was added to a nanowire solution in chloroform and stirred overnight. The solution was then precipitated with acetone and centrifuged, and the supernatant was removed. The precipitate was dried *in vacuo* overnight, and the solid was dissolved in $CDCl_3$. Centrifugation was used to remove insoluble material.

XAS Measurements. The XAS measurements (EXAFS and XANES) were performed at the Canadian Light Source (CLS) on the HXMA (Bi L_3 and L_1 edge) and SXRMB (S K-edge) beamlines. HXMA measurements were performed in transmission mode using commercial bulk Bi_2S_3 powder as a standard and toluene dispersions of nanowires at desired concentrations to obtain optimized EXAFS signals. SXRMB measurements (in a total electron yield) were performed under high vacuum from dropcast chloroform solutions of nanowires and commercial bulk Bi_2S_3 powder as a standard. The EXAFS data were normalized and converted to k and R space with the WinXAS program[20] using standard methods.[21,22] EXAFS fitting was performed using the phase and amplitude functions derived from the Bi_2S_3 bulk EXAFS whose bond distances and coordination numbers were obtained from single crystal X-ray diffraction data.[23] The bulk Bi_2S_3 powder used as the standard was shown to be of high crystallinity and virtually phase pure by Powder X-ray Diffraction (Figure S1). Structural parameters of nanowires such as bond distances and coordination numbers were obtained by a nonlinear least-squares fit of the first-shell EXAFS in *k*-space, which was generated by back-transforming the first-shell FT-EXAFS with an *R* range of 1.6 to 2.8 Å.

XPS Measurements. XPS were acquired at Surface Interface Ontario using a Thermo Scientific Theta Probe utilizing monochromatic Al Kα radiation. High-resolution spectra were acquired on dropcast nanowire films from chloroform with an energy step size of 0.1 eV.

NMR. ^{1}H and ^{13}C NMR spectra were acquired on a 400 MHz Varian Mercury instrument at 25 °C and referenced to the proteo solvent impurity. Concentrations were determined using a method published by Hens et al.[24] Briefly, a known amount of CH_2Br_2 is dissolved in 750 μL of a dispersion of nanowires in d^8-toluene, and the ^{1}H NMR spectrum was collected with an interscan delay of 45 s to make sure full T_1 relaxation occurs. From the relative integrations, a comparison can be made between the concentration of CH_2Br_2 and oleylamine. Variable temperature spectra were acquired on a Varian NMR System 400 between −60 and 55 °C in d^8-toluene and referenced to the proteo solvent impurity.

Results

EXAFS. EXAFS is a phenomenon that results from the absorbance of monochromatic incident X-rays, which cause the ejection of a core electron. Scattering of these photoelectrons by atoms surrounding the central absorbing atom (Bi in this case) results in constructive and destructive interference of the photoelectrons. This interference generates the so-called fine structure in the absorption spectrum. The absorption is plotted as a function of the energy (E) of the incident photons. The resulting spectrum can be converted into a function dependent on the photoelectron wavevector, $\chi(k)$, $k = [2m_e(E - E_0)/\hbar^2)]^{1/2}$, where E_0 is the threshold energy of absorption, by subtracting the nonoscillatory background absorption, $\mu_0(E)$, from the total measured absorption, $\mu(E)$, and normalizing. The *k*-space spectrum can be expressed by the standard EXAFS equation:

$$\chi(k) = S_0^2 \sum_j \frac{N_j F_j(k) S_i(k) e^{-2\sigma_j^2 k^2} e^{-2R_j/\lambda(k)}}{kR_j^2} \sin(2kR_j + \varphi_{ij}(k)) \quad (1)$$

A complete definition of variables is defined in the Supporting Information (Figure S2), while the variables immediately relevant to this discussion are as follows: N_j is the coordination number of the j^{th} atom surrounding the central absorbing atom, R_j is the distance of the j^{th} atom from the central absorbing atom, $F_j(k)$ is the amplitude reduction function of the j^{th} atom, σ_j is the Debye−Waller factor of the j^{th} atom (disorder term), $S_i(k)$ is the amplitude reduction function of the absorbing atom, and $\varphi_{ij}(k)$ is the phase function due to scattering by the j^{th} atom. The *k*-space EXAFS can be converted to distance (R) space by applying a Fourier transform. This process produces a spectrum of the scattering of the photoelectron as a function of the radial distance from the central absorbing atom, with the peaks corresponding to atoms near to the absorbing atom (i.e., chemical bonding).

To gain quantitative information from EXAFS, one must fit the spectrum to solve for the unknown variables such as coordination number and bond distance. Experimental data are usually fit by one of two methods. The first uses an *ab initio* method through a program such as FEFF to simulate the amplitude ($F_j(k)$) and phase ($\varphi_{ij}(k)$) functions.[25] These functions can then be applied to the experimental EXAFS data to determine values such as coordination number and bond distance. A second common approach, and the one used in this article, is to extract the phase and amplitude functions from the EXAFS measurement of a standard sample that is representative of the material under investigation. These functions are then used to determine parameters such as bond distance and coordination number.

Figure 1 shows the k^3-weighted and Fourier Transformed (FT) EXAFS of a dispersion of ultrathin Bi_2S_3 nanowires in toluene and bulk Bi_2S_3 powder for the L_3-edge of Bi.

First, one notices that the *k*-space EXAFS are nearly identical for the Bi_2S_3 bulk and nanowire dispersion. Both the amplitude and periodicity of the *k*-space EXAFS is dependent on the average coordination number of bismuth and the average distance of nearby atoms as described in eq 1. Since the spectra are similar, it demonstrates that the bismuth atoms in both samples are in similar coordination environments. Given the small diameter of the nanowires, there is the possibility of a cluster-like structure for the nanowire core that differs from the bulk crystal; however, the *k*-space EXAFS implies that the local bismuth environment is similar in both samples. The distance space EXAFS (Figure 1b) only clearly shows the first Bi coordination shell, which is seen as the most intense peak in each spectrum. Interestingly, the FT EXAFS shows a greater intensity for the nanowire solution, which suggests a larger coordination number than the bulk. This is unexpected as nanocrystals typically have lower coordination numbers due to the large amount of surface atoms (high surface:volume ratio), which contain incomplete coordination spheres and dangling bonds.

(20) Ressler, T. *J. Synchrotron Radiat.* **1998**, *5*, 118–122.
(21) Zhang, P.; Sham, T. K. *Phys. Rev. Lett.* **2003**, *90*, 245502.
(22) Zhang, P.; Zhou, X. T.; Tang, Y. H.; Sham, T. K. *Langmuir* **2005**, *21*, 8502–8508.
(23) Lukaszewicz, K.; Stepien-Damm, J.; Pietraszko, A.; Kajokas, A.; Grigas, J. *Pol. J. Chem.* **1999**, *73*, 541–546.
(24) Moreels, I.; Martins, J. C.; Hens, Z. *ChemPhysChem* **2006**, *7*, 1028–1031.
(25) Ankudinov, A. L.; Ravel, B.; Rehr, J. J.; Conradson, S. D. *Phys. Rev. B* **1998**, *58*, 7565–7576.

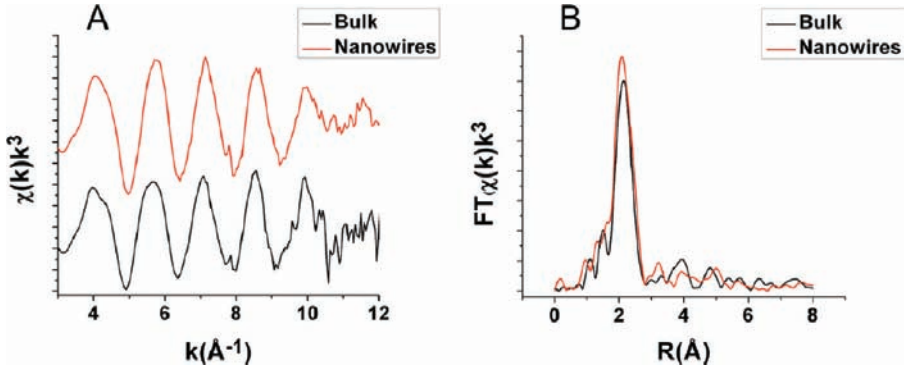

Figure 1. Bi L_3-edge (A) *k*-space and (B) distance space of Bi_2S_3 bulk and ultrathin nanowires in toluene.

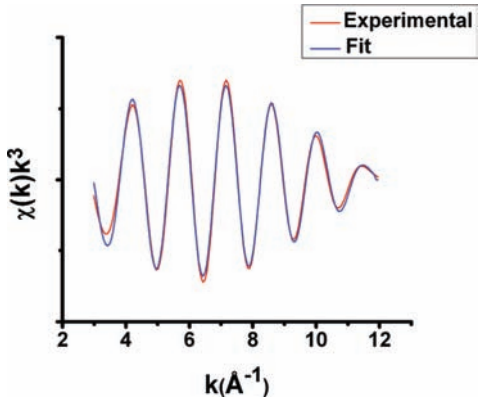

Figure 2. Backtransformed first shell *k*-space of ultrathin Bi_2S_3nanowires in toluene and experimental fit.

Table 1. EXAFS Fitting Results for Bi L_3 Edge of Bi_2S_3 Bulk and Ultrathin Nanowires in Toluene[a]

Sample	*N*	*R* [Å]	σ^2	ΔE_0
Nanowires	4.0 ± 0.2	2.667 ± 0.003	0.0017 ± 0.0004	0.9 ± 0.3
Bulk	3.0	2.682	N/A	N/A

[a] The coordination number, *N*, and average bond distance, *R*, for the bulk were obtained from ref 23.

The phase and amplitude functions for bulk Bi_2S_3 were obtained by using crystallographic data for the average first shell coordination number, $N = 3$, and the average bond length, $R_{average} = 2.682$ Å.[23] An average bond distance was used, as there are two crystallographically distinct bismuth atom sites that form several Bi−S bonds of slightly different lengths, which can be hardly distinguished in EXAFS. Our use of the experimentally determined phase and amplitude functions is justified by the similarity of the *k*-space EXAFS of bulk Bi_2S_3 and solution-phase nanowires. These functions were then plugged into eq 1, which was then used to fit the nanowire solution EXAFS and determine the average coordination number and bond distance. The nonlinear least-squares fit was performed on the k^3 weighted EXAFS of the nanowires obtained by backtransforming the first coordination shell in the distance space EXAFS (~1.6−2.8 Å) into *k*-space. The backtransformed experimental *k*-space and fitted spectra are shown in Figure 2, and the parameters, including the bond distance (*R*), coordination number (*N*), Debye−Waller factor (σ^2), and corrected threshold energy (ΔE_0), are presented in Table 1.

The fitting results show a statistically significant bond length contraction of 0.015 Å, which is expected for a nanocrystal and has been attributed to a surface energy minimization effect.[26] However, the increase of the coordination number from three to four is not expected and to our knowledge is without precedent in nanocrystal systems.

XANES and XPS. XANES and XPS can both provide detailed information on oxidation states and chemical species based on characteristic absorption (XANES) and binding energies (XPS) of core electrons. The Bi L_1- and S K-edge XANES were acquired on colloidal dispersions of nanowires and dropcast films, respectively, while the Bi 4f, S 2s, and N 1s XPS were acquired on dropcast films. Spectra are recorded under high vacuum for all samples with the exception of the Bi L_1-edge, which necessitates the use of dry films. Bulk Bi_2S_3 powder was used in the XANES measurements as a standard sample. XPS has been performed previously on Bi_2S_3 crystals, and the literature data were used as a reference.[27]

The S K-edge XANES is shown in Figure 3a, along with the S 2s XPS (Figure 3b). The S K-edge deviates very little from that of bulk Bi_2S_3. The main absorption edge is similar compared to bulk Bi_2S_3 but consists of a doublet instead of a singlet. One peak is likely due to Bi−S species, while the second we attribute to polymeric sulfur or cyclooctasulfur (S_8), a byproduct of the reaction that is difficult to remove during purification. Both S_8 and polymeric sulfur are observed as a doublet with virtually identical spectra, with a large peak centered at 2470 eV and a broad peak between 2476 and 2480 eV at approximately 40% the intensity of the peak at 2470 eV.[28] Both of these peaks are observed in the nanowire spectrum. However, SO_x species are also found at ~2480 eV and are observed as a sharp singlet.[27] Given that the nanowire spectrum contains two main peaks, with the peak at ~2480 eV at a higher intensity than the lower energy peak, we suggest that SO_x species exist along with S_8/polymeric sulfur. The sharpness and relative intensity of the peak at 2480 eV is not consistent with S_8/polymeric sulfur, as the peak would be expected to be lower in intensity than the peak at 2470 eV and broad. Therefore, we suggest that SO_x species are the dominant contributor to the peak at 2480 eV.

The S 2s XPS can be deconvoluted into two Gaussian peaks (Figure 3b). The lower energy peak is at 225 eV, consistent with Bi−S species as observed by Grigas et al.[26] A second peak at higher energy is observed at 227 eV. S_8 is expected at 228 eV while metal sulfites ($M_x(SO_3)_y$) are typically found at ~230 eV.[26,29] Based on the S K-edge data, it is likely that the peak at

(26) Marcus, M. A.; Andrews, M. P.; Zegenhagen, J.; Bommannavar, A. S.; Montano, P. *Phys. Rev. B* **1990**, *42*, 3312–3316.
(27) Grigas, J.; Talik, E.; Lazauskas, V. *Phys. Status Solidi* **2002**, *232*, 220–230.
(28) Prange, A.; Chauvistré, R.; Modrow, H.; Hormes, J.; Trüper, H. G.; Dahl, C. *Microbiology* **2002**, *148*, 267–276.

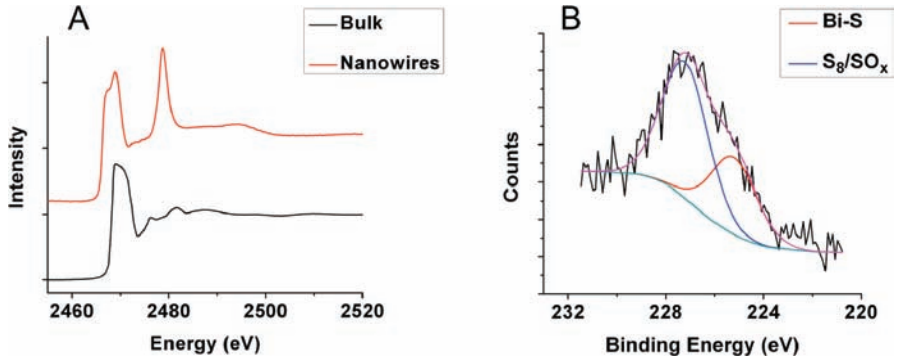

Figure 3. (A) S K-edge XANES of Bi_2S_3 bulk and ultrathin nanowires in toluene and (B) fitted S 2s XPS of ultrathin Bi_2S_3 nanowires.

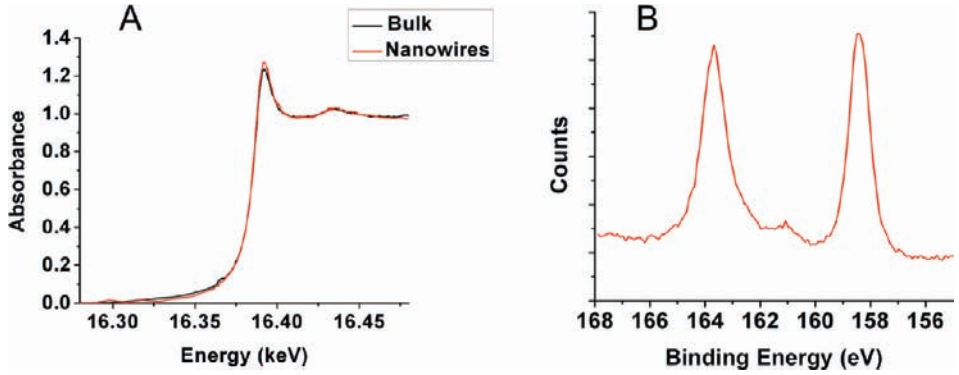

Figure 4. (A) Bi L_1-edge XANES of Bi_2S_3 bulk and ultrathin nanowires and (B) Bi 4f XPS of ultrathin nanowires.

227 eV is due to a combination of both SO_x species, where $x < 3$ (that differs from a metal sulfite salt), and S_8. However, the low signal-to-noise ratio makes an exact assignment unreliable. Nonetheless, the S 2s XPS data appear to be consistent with the S K-edge assignment.

We similarly probed the Bi L_1-edge, although this experiment could be measured in solution as the X-rays at the absorption edge are much higher in energy and can more easily penetrate the solvent. The spectra are shown in Figure 4, along with the Bi 4f XPS. Once again, the bulk and nanowire sample are similar in both the shape of the edge and onset of absorption, supporting the conclusion that the nanowires adopt a structure similar to that for the bulk. However, the white line (the most intense peak after the absorption edge) of the nanowire sample is significantly more intense. This has been observed in the L_3-edge XANES of small Pd nanoparticles and is attributed to a higher unoccupied density of states (DOS) of d-electrons.[30] In the case of the nanowires, the L_1 transition is from a 2s to 6p orbital, which means we can attribute this effect to a decreased 6p DOS.[31] The Bi 4f XPS was acquired to determine if any Bi−O species exist. The Bi 4f XPS confirms that no Bi−O species are present as the 4f binding energy of Bi_2O_3 is expected at 166 and 161.5 eV, of which there is no sign of in the nanowire spectrum.[32] The small peak observed at 161.5 eV is due to the S 2p electrons. Along with the almost identical absorption edges in the Bi L_3 and L_1 spectra compared to the bulk, we suggest that surface SO_x species are responsible for the increased L_1-edge white line of the nanowires. The presence of surface Bi−SO_x species would cause a decrease in the Bi 6p DOS due to the electron-withdrawing oxygen atoms, which is likely responsible for the increased white line.

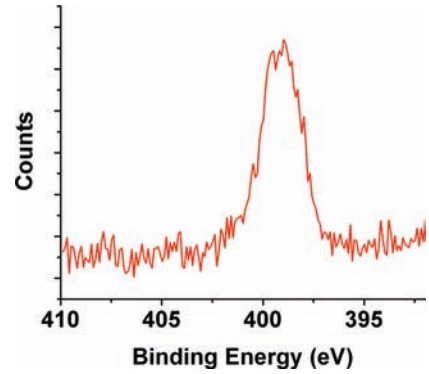

Figure 5. N 1s XPS of a dropcast solution of ultrathin Bi_2S_3 nanowires.

The N 1s XPS, shown in Figure 5, has a broad peak centered at ~399 eV. Primary amines are expected at ~399 eV, with protonated amines found at 402 eV.[33] The N 1s XPS of the nanowires is quite broad suggesting more than one nitrogen species is present. Attempts to deconvolute the peak produced results that were not unequivocal. Previous studies on amine capped Au nanoparticles show that the N 1s binding energy barely shifts to higher energy upon binding to surface Au atoms (~0.1−0.2 eV).[34] This makes it difficult to distinguish the contribution of bound and free amine species, although it is likely that both are present in the spectrum.

(29) Zingg, D. S.; Hercules, D. M. *J. Phys. Chem.* **1978**, *82*, 1992–1995.
(30) Cook, S. C.; Padmos, J. D.; Zhang, P. *J. Chem. Phys.* **2008**, *128*, 154705.
(31) Charnock, J. M.; England, K. E. R.; Henderson, C. M. B.; Mosselmans, J. F. W.; Pattrick, F. A. D. *J. Phys. IV* **1997**, *7*, 1137–1138.
(32) Ismail, F. M.; Hanafi, Z. M. *Z. Phys. Chem. (Leipzig)* **1986**, *267*, 667.
(33) Ratner, B. D.; Castner, D. G. *Biomaterials* **1990**, *11*, 143–146.
(34) Kumar, A.; Mandal, S.; Selvakannan, P. R.; Pasricha, R.; Mandale, A. B.; Sastry, M. *Langmuir* **2003**, *19*, 6277–6282.

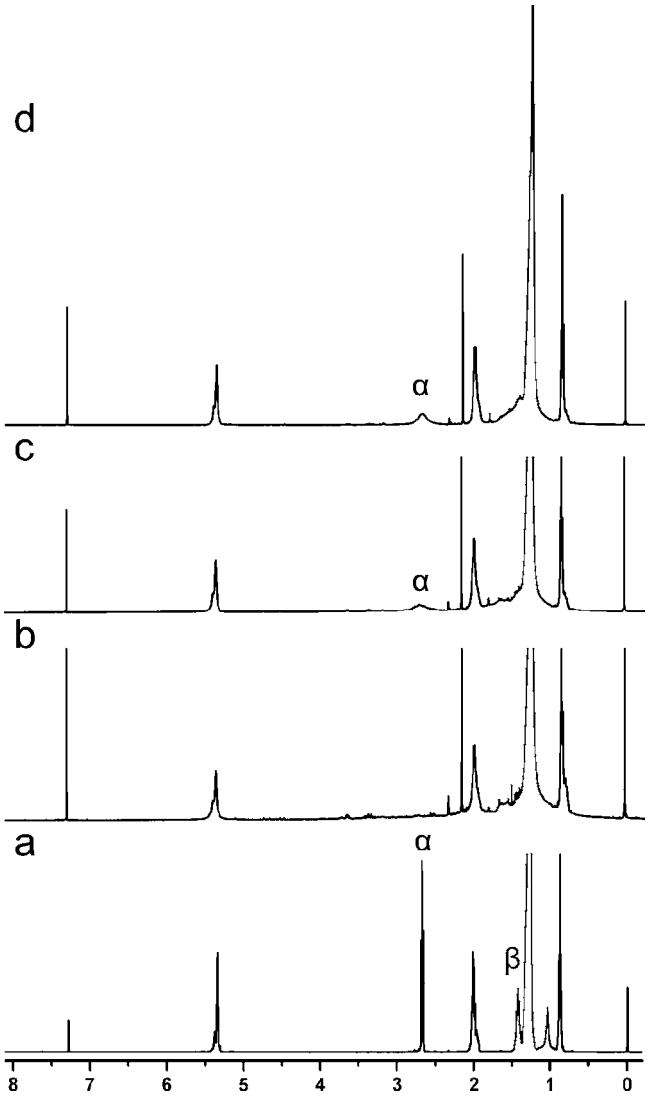

Figure 6. ^{1}H NMR of (a) free oleylamine, (b) purified oleylamine capped Bi_2S_3 nanowires, and (c−d) nanowires with additional oleylamine in $CDCl_3$.

From the XPS results, atomic percentages were calculated (Figure S3). The measured S/Bi ratio is 2.5, which is higher than the expected 1.5 for bulk Bi_2S_3. However, removal of all impurities such as polysulfide/sulfur is quite difficult to do without compromising colloidal stability. As such, an exact S/Bi stoichiometry is difficult to calculate and the value shown is likely to include a sulfur impurity based on the S K-edge XANES. The N/Bi ratio was calculated to be 4.2, indicating that there is an excess of oleylamine compared to Bi even after purification.

NMR Results. ^{1}H and ^{13}C NMR spectra were acquired to study the nature of stabilization of oleylamine capping ligands. Typical ^{1}H NMR spectra with varying degrees of additional oleylamine, along with free oleylamine, are shown in Figure 6. Two main differences are observed between free oleylamine and oleylamine capped ultrathin nanowires. The first is the lack of signal due to the protons bonded to the carbon atoms in alpha and beta positions with respect to the nitrogen. This effect has been observed in ruthenium nanoparticles capped by hexadecylamine (along with many other nanocrystal/ligand combinations) and is attributed to chemical shift distribution due to magnetically inequivalent environments and short T_2 relaxation times caused by slow tumbling of the particles in solution.[35,36] These effects are especially pronounced for the protons near the surface of the nanocrystal. The second feature is the presence of a sharp singlet at 2.2 ppm, which we attribute to residual acetone based on the chemical shift in both the ^{1}H and ^{13}C NMR spectra. The acetone cannot be easily removed even after being left under vacuum overnight; however, its signal is sharp indicating that it does not bind to the nanowires.

Table 2. Nitrogen to Bismuth Ratios Calculated by NMR/UV−vis Spectra and XPS for a Purified Dispersion of Ultrathin Bi_2S_3 Nanowires

Method	[N]	[Bi]	[N]/[Bi]
NMR/UV−vis	66 mM	15.1 mM	4.4
XPS	2.30%	0.54%	4.3

If additional oleylamine is added to a solution of purified nanowires, peaks corresponding to the alpha and beta protons begin to appear, but they remain much broader than those of free oleylamine. The lack of a distinct signal from free and bound oleylamine indicates that the exchange is likely fast on the NMR time scale. Indeed, the N 1s XPS also suggests the presence of free and bound oleylamine. The ^{13}C NMR spectra also showed similar results and are shown in Figure S4.

To determine the Bi/N ratio, we used a concentration standard, CH_2Br_2, to determine the amount of oleylamine present in the sample. Hens et al. used this method to determine exact concentrations of ligands in solution.[24] In our case, the integration of the methyl resonance of oleylamine was compared to the integration of CH_2Br_2. The previously reported extinction coefficient allowed us to determine the concentration of Bi atoms based on the UV−vis absorbance of the nanowires.[6] The result for the NMR/UV−vis calculation is a ratio of 4.4 N/Bi and is shown in Table 2 along with the atomic ratio of Bi/N from XPS data. Both methods show excellent agreement. However, the exact integration of the methyl group is difficult as it overlaps slightly with the methylene backbone (Figure S5). Nonetheless, both XPS and NMR confirm that there is an excess of oleylamine even after purification.

To further understand the surface chemistry of the nanowires, we performed ligand exchange experiments. Oleylamine provides a good NMR handle in the form of the olefinic protons/carbons and allows the facile observation of ligand exchange with saturated ligands, provided that good colloidal stability is maintained. We performed the ligand exchange with hexadecylamine, a primary amine virtually identical to oleylamine, but lacking a double bond. Exchange was performed by simply stirring an excess of hexadecylamine in a nanowire solution overnight and purifying with one precipitation/redispersion. Figure 7 shows that ligand exchange is quantitative (see Figure S6 for ^{13}C NMR). The alpha and beta protons are extremely broad and weak, indicating coordination of the amine to the surface of the nanowires. Moreover, the olefinic protons at 5.4 ppm are no longer visible, nor are the protons alpha to the double bond at 2 ppm. As with oleylamine-capped nanowires, the chemical shifts change very little between free and bound amine. Presumably, both ligands have a similar affinity for the nanowire surface as they are both primary alkylamines; however, the large excess of hexadecylamine drives the exchange through mass action.

(35) Pan, C.; Pelzer, K.; Philippot, K.; Chaudret, B.; Dassenoy, F.; Lecante, P.; Casanové, M.-J. *J. Am. Chem. Soc.* **2001**, *123*, 7584–7593.
(36) Badia, A.; Cuccia, L.; Demers, L.; Morin, F.; Lennox, R. B. *J. Am. Chem. Soc.* **1997**, *119*, 2682–2692.

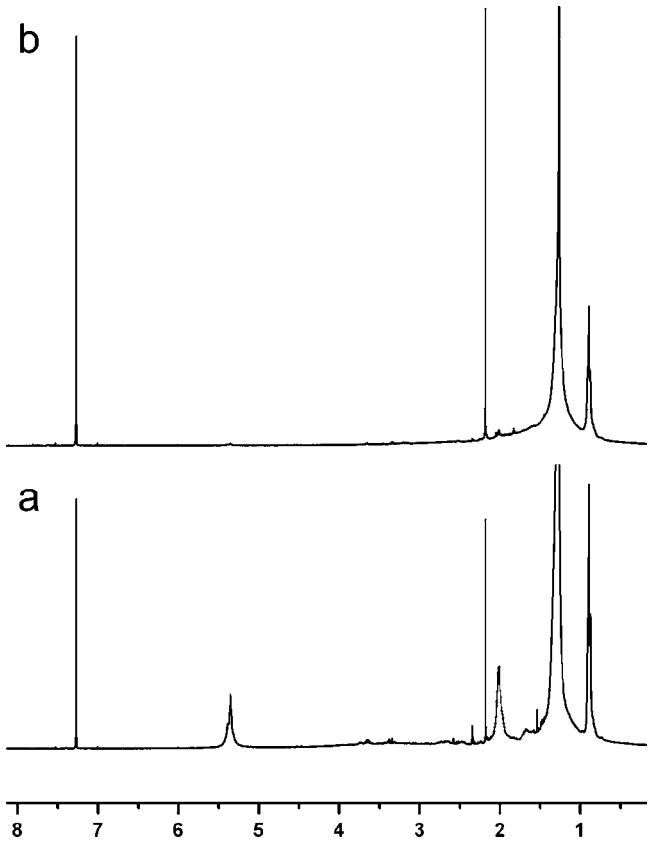

Figure 7. ^{1}H NMR spectra of (a) oleylamine capped ultrathin Bi_2S_3 nanowires and (b) hexadecylamine exchanged ultrathin Bi_2S_3 nanowires in $CDCl_3$.

Variable temperature (VT) NMR experiments were also performed with the idea of studying the dynamic exchange of surface bound and free oleylamine ligands. Previous work by Hens et al. studied trioctylphosphine oxide (TOPO)/trioctylphosphine (TOP) adsorption/desorption from the surface of InP nanocrystals at room temperature.[24] The exchange observed in this case was slow on the NMR time scale, which allowed the resolution of distinct methyl peaks for adsorbed and free TOPO/TOP. In the case of the ultrathin Bi_2S_3 nanowires, ligand exchange between free and bound oleylamine is fast on the NMR time scale, leading to an averaged peak. In an attempt to slow down the exchange process, we decreased the temperature of a nanowire dispersion in d^8-toluene with an additional 7 μL of oleylamine. Interestingly, decreasing the temperature to -60 °C was not enough to slow down sufficiently the exchange between free and bound oleylamine as the alpha proton peak remained unchanged (Figure S7). Although we could not calculate an exact value for the activation energy as the coalescence temperature was not reached, this experiment shows that the kinetic barrier for exchange is low compared to other ligand/nanocrystals systems.

Discussion

The EXAFS, XANES, and XPS characterization confirmed that the atomic structure of the inorganic core of the ultrathin Bi_2S_3 nanowires is indeed consistent with the one of bismuthinite, as previously suggested by Rietveld refinement of PXRD diffractograms.[6] Nonetheless, the fit of the EXAFS data highlighted that, beside the small but significant (0.5%) contraction in the average nearest neighbor bond lengths, the bismuth atoms in the nanowires experience an average coordination number (4) which is remarkably higher than that in bulk bismuthinite (3). This observation apparently contradicts the common understanding of nanocrystalline systems as having decreased coordination numbers due to dangling bonds.

To understand this observation, we must look at the crystal structure of Bi_2S_3, which is shown in Figure 8. The bulk structure is characterized by two crystallographically distinct bismuth sites and three crystallographically distinct sulfur sites (Figure 8a). The seven Bi−S distances are all between ∼2.5 and ∼3.3 Å. The three shorter distances (between 2.593 Å and 2.745 Å) for each bismuth site can be considered to be *intrachain* bonds with stronger covalent character that make up Bi_2S_3 chains elongating along the *c*-axis of the crystal lattice (Figure 8b). These bonds are the ones observed by EXAFS. The chains interact with each other via weaker *interchain* interactions, which are represented by the four remaining Bi−S distances. The anisotropy of the crystal structure is reflected in the lattice parameters ($a = 11.193$ Å, $b = 11.345$ Å, $c = 3.994$ Å, space group *Pbnm*) and is one of the purported reasons of the pronouncedly anisotropic crystal habit of Bi_2S_3.[37] Given that the nearest neighbor shell was chosen for the fitting, only the *intrachain* "covalent" bonds contribute to the fitted values of the EXAFS spectrum, as the nearest *interchain* distance is 2.96 Å, 0.16 Å outside of the fitted area.[23] In other words, the weaker interactions between each chain are not "seen" by the EXAFS in our fit. As such, each chain can essentially be envisioned as a distinct unit, whether on the surface or in the core. In the bulk, we see a first shell coordination number of 3 for all bismuth atoms except those that terminate the chains, which possess a coordination number of 2. The high aspect ratio of the Bi_2S_3 nanowires ensures that the bismuth atoms at the chain termini contribute very little to the average coordination number of the nanowires (see Figure S8 for TEM). Thus, the first shell coordination number of Bi due to Bi−S bonds is 3.

Figure 9 shows two potential structural models of the ultrathin Bi_2S_3 nanowires. These are the only models that are (i) consistent with the observed 1.6 nm diameter by TEM and (ii) formed without breaking *intrachain* covalent bonds. These models are based on the bulk structure of bismuthinite and, as such, do not take into account the surface reconstruction that would likely draw Bi atoms to the surface to interact with the ligands to expand their coordination.[4] The black and blue spheres represent easily accessible Bi atoms, the orange and pink spheres represent Bi atoms which are accessible, while the yellow spheres represent inaccessible Bi atoms.

A Bond Valence Sum (BVS) analysis was carried out to assess (i) the missing valency at the accessible bismuth surface sites and (ii) the most energetically favorable structure. In this analysis the valence of a cation is measured as the sum of the strengths of the bonds it forms. The practical application requires the definition of a bond strength−bond length correlation curve for a given cation−anion pair that has been derived by analyzing ∼15 000 cation environments from the Inorganic Crystal Structure Database, by Brown and Altermatt.[38a,b] This work focused on M−O and M−S pairs, which allows one to assign a bond valence value to an observed bond length (see Figure S9 for Bi−S curve). The advantage of BVS, when compared

(37) Wang, Y.; Chen, J.; Wang, P.; Chen, L.; Chen, Y. B.; Wu, L. M. *J. Phys. Chem. C* **2009**, *113* (36), 16009–16014.
(38) (a) Altermatt, D.; Brown, I. D. *Acta Crystallogr., Sect. B* **1985**, *41*, 240–244. (b) Altermatt, D.; Brown, I. D. *Acta Crystallogr., Sect. B* **1985**, *41*, 244–247.

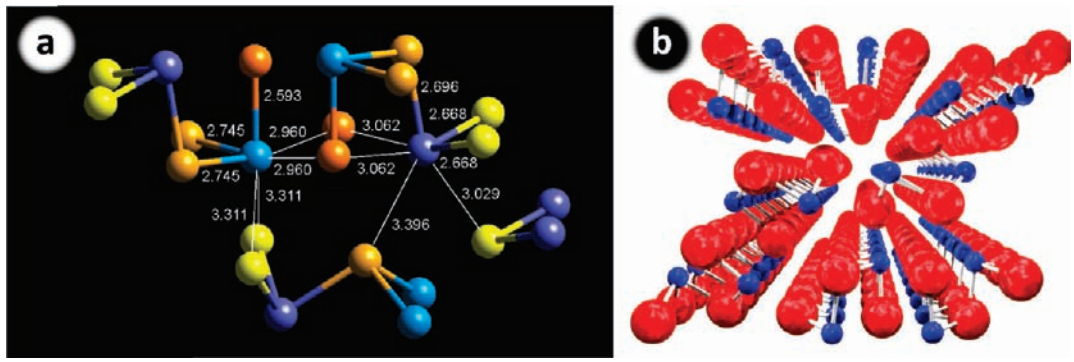

Figure 8. Crystal structure of Bi_2S_3 based on ref 23. (a) 3D representation of the environments of the two bismuth sites (light blue and dark blue); the three sulfur sites are shown with different tones of yellow; the cylinders represent the three shortest Bi−S distances which are attributed to the bonds with the stronger covalent character; the numbers represent the corresponding Bi−S distances (in Å). (b) 3D perspective representation of the bismuthinite structure portrayed along the *c*-axis of the unit cell; the cylinders represent the "covalent" bonds.

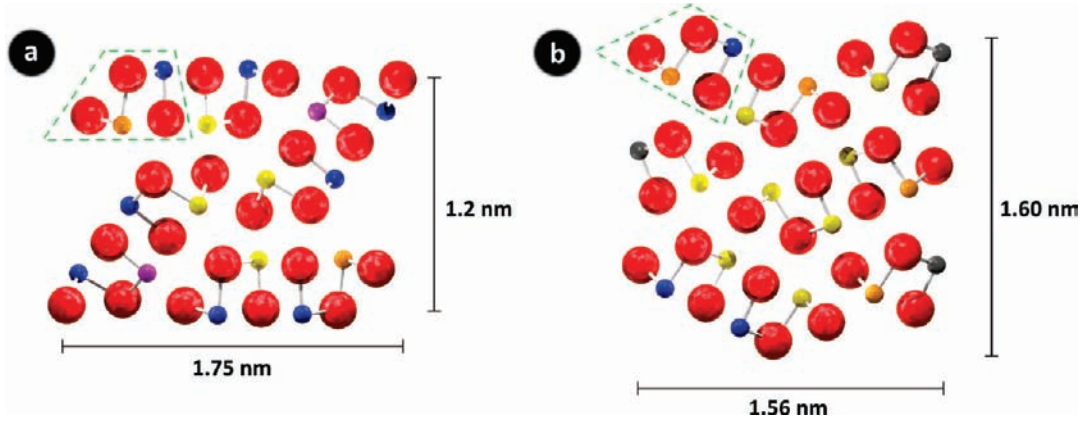

Figure 9. Comparison of the cross section of the two possible structural models for the ultrathin Bi_2S_3 nanowires. In both panels we use the following color scheme: the sulfurs are red, easily accessible bismuths are black and blue, less accessible bismuths are orange and pink, while inaccessible bismuths are indicated in yellow. A) Original model composed of 8 Bi_2S_3 chains (one such chain is identified by a green dashed outline) B) Alternative model composed of 9 Bi_2S_3 chains. Both models are exact subsets of the bismuthinite lattice "cleaved" along the *c* axis of the structure and the weaker interchain bonds. These models do not depict lattice compression, strain, or surface reconstruction.

to more sophisticated methods of analysis like Charge Distribution Analysis (CDA), is that it can be applied to fragments of the crystal lattice. In this case we apply it to the surface of the nanowires. For the first proposed model (Figure 9a), the valence of the inaccessible Bi atoms can be estimated from BVS to be 3.169 and 3.154 for the two inequivalent sites. The easily accessible surface bismuths (shown in blue in Figure 9a) show a valence of 2.773 and 2.884. The less accessible bismuth site (orange in Figure 9a) shows a valence of 2.880. The remaining accessible bismuth site (pink in Figure 9a) shows a full valence and, as such, can be considered to have no "dangling" bonds. This analysis obviously assumes that the bond distances within the core of the nanowire are essentially analogous to the ones in the bulk, which is most likely not exactly true due to lattice compression, strain, and surface reconstruction. The second model (Figure 9b), even if characterized by an equivalent number of Bi atoms exposed at the surface, is much more inhomogeneous in terms of surface energy. In fact, BVS analysis shows that it contains three accessible bismuth atoms (black color) that have a valence of only 2.186, while the other atoms range from 2.773 to 3.062. Such inhomogeneities in surface energy seem unlikely as they would likely result in a reconstruction of the surface through dissolution and regrowth. In addition, while the second model has two additional bulk bismuth atoms, it has a lower average bismuth valence (2.90 instead of 2.96), suggesting a higher free energy. We therefore propose that Figure 9a represents the most reliable model based on BVS analysis. According to this model, up to 75% of Bi atoms are accessible at the surface.

The additional coordination of surface bismuth atoms can only occur with oxygen, sulfur, or nitrogen from oleylamine. Surface Bi—O species can be excluded based on the lack of any Bi—O species in the Bi 4f XPS. The atomic ratios determined from XPS show an increased S/Bi ratio, suggesting the possibility of S^{2-} or SO_4^{2-} coordination of the surface bismuth atoms. While SO_x species were not unequivocally observed in the S 2s XPS (Figure 3b), the S K-edge XANES (Figure 3a) does show their presence. Nonetheless, if additional S^{2-} or SO_4^{2-} would be bound to the surface of the nanowires, the net charge of the inorganic core of the nanowire would be negative. Kumar et al. found that Au nanoparticles synthesized in amine surfactants contain surface $AuCl_4^-$ ions that are charge balanced by alkylammonium cations, which were detected by N 1s XPS.[39] Similarly, PbS quantum dots synthesized by our group in oleylamine show a Pb-rich surface, and the counterion was found to be composed of a monolayer of Cl^- ions originating from the lead precursor, $PbCl_2$.[40] If the surface of our nanowires is rich in sulfide or SO_x anions, the charge balancing cation

(39) Kumar, A.; Mandal, S.; Selvakannan, P. R.; Pasricha, R.; Mandale, A. B.; Sastry, M. *Langmuir* **2003**, *19*, 6277–6282.
(40) Cademartiri, L.; Bertolotti, J.; Sapienza, R.; Wiersma, D. S.; von Freymann, G.; Ozin, G. A. *J. Phys. Chem. B* **2006**, *110* (2), 671–673.

could only be a protonated oleylamine. Since both the N 1s XPS (Figure 5) and $^{1}H/^{13}C$ NMR (Figures 6 and S6) showed no ammonium species, the increased Bi coordination number as well as the excess sulfur atoms cannot be attributed to the coordination by excess sulfide or SO_x. The SO_x species, if present, must then be formed by the oxidation of surface sulfurs. This oxidation would only add oxygens to the Bi_2S_3 stoichiometry of the wires and would not add charge to the surface of the nanowires. The negative charges introduced by the oxide ions would be in fact compensated by a change in the oxidation state of the surface sulfur bound to them. A dative interaction between the primary amine and the surface sulfur atoms was considered. To our knowledge, there are no examples of characterized neutral amine-sulfide adducts in the literature (our XPS characterization demonstrates that the amines are neutral), with the exception of so-called charge transfer complexes between electropositive sulfur atoms (e.g., SO_2) and amines.[41] In those complexes the electropositive sulfur accepts electrons from the amine nitrogen. In the case of Bi_2S_3, the sulfur atoms possess a significant negative charge due to unequal sharing of electrons between Bi and S. As such, electron donation from an electron-rich nitrogen to a negatively charged sulfur seems thermodynamically implausible. Nitrogen cannot become hypervalent as occurs with phosphine chalcogenides ($R_3P{=}S$), which have been proven to stabilize nanocrystals through partial interaction with the chalcogenide sites.[42] Moreover, while the Bi—N interaction is expected to be much stronger on its own, it is possibly stabilized by hydrogen bonding between the amine hydrogens and adjacent sulfur atoms, making it effectively a multivalent interaction. In the case of a N—S interaction, the hydrogen atoms on the amine would be pushed near the electropositive Bi atoms, an energetically unfavorable state. If such an interaction were even possible, it seems certain that, in a competitive situation, the Bi—N interaction would vastly prevail over a N—S interaction. Based on this logic, the lack of literature precedent, and the lack of evidence from our FT-IR, NMR, and the N 1s XPS experiments for such an N—S interaction, we believe that the Bi—N interaction is dominant and that, apart from H-bonding with surface S-atoms, an eventual N—S interaction could be disregarded.

We therefore propose that the increased coordination number is due to the dative Bi—N metal—ligand bonds between oleylamine and the surface Bi atoms. The ultrathin Bi_2S_3 nanowire model shown in Figure 9 has ~75% of Bi atoms potentially accessible to the ligands. If every accessible Bi atom would bind to one oleylamine molecule, the average coordination number (assuming full coverage) would be 3.8, which is within the error of the coordination number as calculated by EXAFS. However, there is plausibly also a contribution from dual coordination of the most accessible Bi surface atoms (shown in blue in Figure 9). If this is considered, the maximum average coordination number for Bi that could be accounted by our model (assuming full amine coverage) would be 4.2.

If Bi atoms are bound with both S and N, we might expect to see two distinct peaks in the distance space EXAFS, while in fact only one species is observed in the first coordination shell between 1.6 and 2.8 Å. However, nitrogen and sulfur are too similar in atomic mass and, as such, they would not produce distinct peaks. Similar observations have been made by Alivisatos et al., where CdS nanocrystals capped by pyridine/water did not show distinct peaks for Cd—S and Cd—N/O species, but Cd—N/O species were required to explain the coordination number that was equivalent to the bulk.[43] In fact, the fitted data for CdSe in the same study suggested that up to two pyridine/water molecules were coordinated to each surface Cd atom. Moreover, the Bi—N bonds would likely overlap with the Bi—S bonds in the distance space EXAFS. Average Bi—N bond lengths in coordination complexes between amines and Bi atoms are 2.4—2.75 Å, in good agreement with the average nearest neighbor bond length of 2.667 Å as determined by EXAFS.[44a—d] If the Bi—N bond length was substantially shorter, a larger contraction of the average bond length in the nanowire sample would be expected, especially if 75% of Bi atoms were interacting with oleylamine.

BVS analysis was further applied to determine (i) the effect of amine coordination on the valence and (ii) the plausibility of double amine coordination. Brese and O'Keefe extended the work of Brown and Altermatt to include M—N pairs (see Figure S10 for Bi—N curve).[45] The nitrogen coordination should provide between 0.27 and 0.4 valence units to compensate for the missing valence. This would correspond to a Bi—N bond length between 2.56 and 2.71 Å, which is within the EXAFS distance range. Single coordination of surface bismuth atoms by an amine satisfies the valence, by giving each Bi a valence near 3 (the bulk value). A double coordination of the most accessible bismuth surface atoms would result in either (i) Bi—N bond lengths slightly exceeding 2.8 Å, barely outside of the EXAFS range, or (ii) slight overbonding conditions where the surface bismuths would have a slightly larger valence than that in the bulk. However, we must consider that besides the inevitable errors in using bulk structure libraries to determine BVS values for a nanoscale material, this analysis does not account for (i) the interaction between bound amines, (ii) the potentially favorable hydrogen bonding between amine protons and sulfur atoms next to the Bi—N interaction, and (iii) the surface reconstruction which would plausibly pull the bismuth cation from the surface, decreasing the strength of the Bi—S bonds, and making a double coordination more favored.

Figure 10 shows the model of possible geometries of the oleylamine coordination to surface Bi atoms. Our model shows the interaction of less accessible purple and orange Bi atoms with one amine and the interaction of blue accessible Bi atoms with two amines. The model is based on the one shown in Figure 9a, using Bi—N bond lengths between 2.56 and 2.71 Å, and covalent radii of atoms from the literature.[46] Only the first carbon atom on oleylamine molecules is shown for clarity.

Sterics are also expected to play an important role in determing whether or not two oleylamine molecules can interact with a surface Bi atom. Coordination complexes of Bi(III) exist in which Bi can be up to 9-coordinate, using multidentate ligands containing N and O donors.[44c,d] Numerous examples of 8-coordinate Bi(III) exist including those which possess nitrogen

(41) Wong, M. W.; Wiberg, K. B. *J. Am. Chem. Soc.* **1992**, *114*, 7527–7535.
(42) Jasieniak, J.; Mulvaney, P. *J. Am. Chem. Soc.* **2007**, *129*, 2841–2848.
(43) Marcus, M. A.; Brus, L. E.; Murray, C.; Bawendi, M. G.; Prasad, A.; Alivisatos, A. P. *Nanostruct. Mater.* **1992**, *1*, 323–335.
(44) (a) Stavila, V.; Davidovich, R. L.; Gulea, A.; Whitmire, K. H. *Coord. Chem. Rev.* **2006**, *250*, 2782–2810. (b) Boyle, T. J.; Pedrotty, D. W.; Scott, B.; Ziller, J. W. *Polyhedron* **1998**, *17*, 1959–1974. (c) Stewart, C. A.; Calabrese, J. C.; Arduego, A. J., III. *J. Am. Chem. Soc.* **1985**, *107*, 3397–3398. (d) Luckay, R.; Reibenspies, J. H.; Hancock, R. D. *J. Chem. Soc., Chem. Commun.* **1995**, 2365–2366.
(45) Brese, N. E.; O'Keeffe, M. *Acta Crystallogr., Sect. B* **1991**, *47*, 192–197.
(46) Cordero, B.; Gómez, V.; Platero-Prats, A. E.; Revés, M.; Echeverría, J.; Cremades, E.; Barragán, F.; Alvarez, S. *Dalton Trans.* **2008**, 2832–2838.

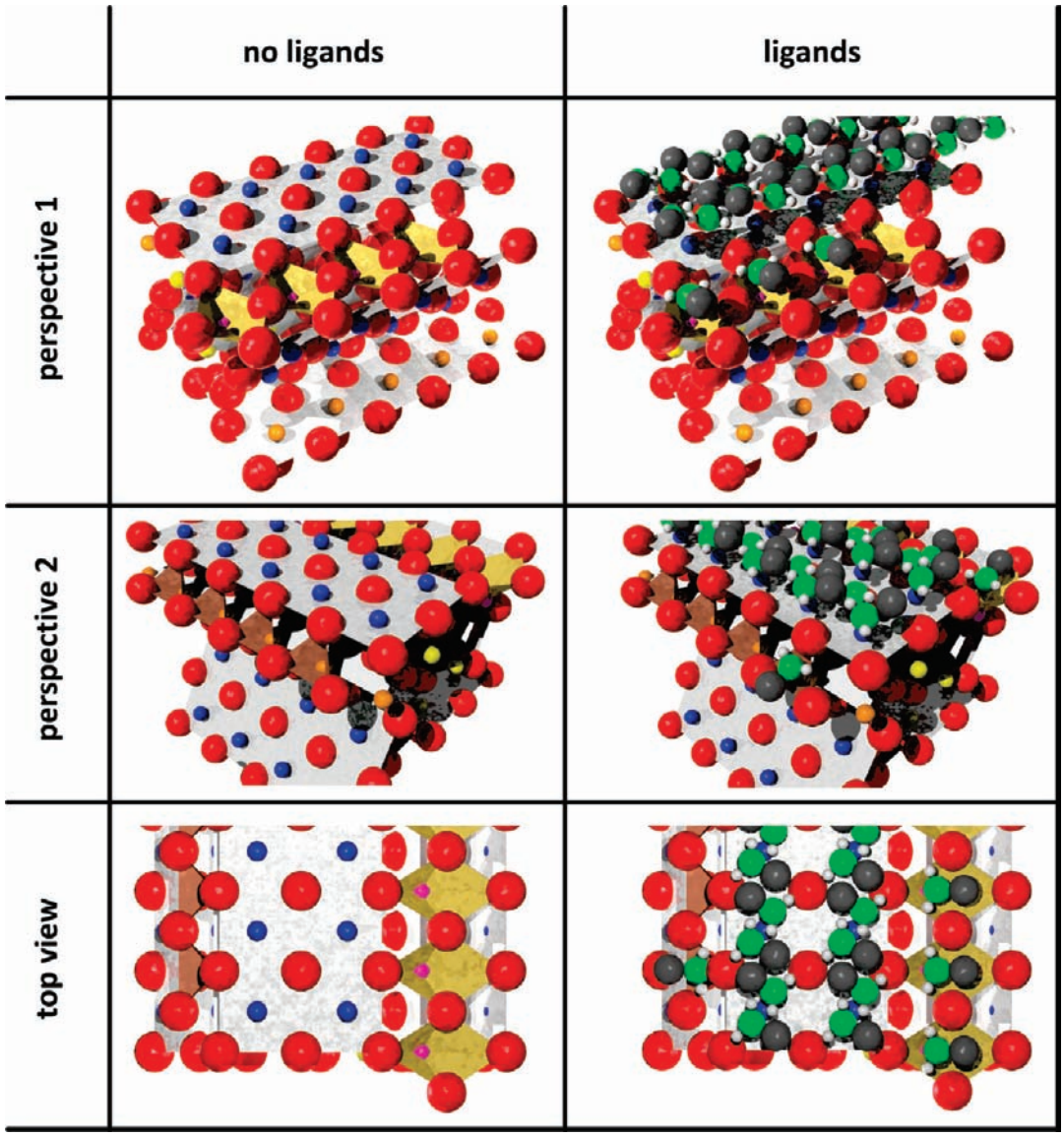

Figure 10. Proposed structure of ultrathin Bi_2S_3 nanowires (L) without and (R) with amine interaction with surface Bi atoms. Green = nitrogen, dark gray = carbon, white = hydrogen. The structure is visualized in different perspectives for convenience. The relative geometry of the accessible bismuth atoms is highlighted by gray ribbons. The geometry surrounding the less accessible bismuth atoms (pink and orange) is highlighted respectively by gold and copper colored cavities.

containing ligands such as pyridine, secondary alkylamines, and methylimidazole.[44a,b] These studies indicate that Bi(III) compounds can easily accommodate large coordination numbers, including amines as ligands. Primary amines also possess a relatively small cone angle of 106°, which makes them less bulky than secondary amines (125° cone angle) and not significantly more bulky than pyridine or methylimidazole.[47] This shows that if two pyridine/several secondary amine molecules can interact with an 8-coordinate Bi atom, a 5-coordinate surface Bi atom with two oleylamine molecules is sterically possible. Moreover, oleylamine is substantially less bulky than typical ligands used in nanocrystals such as TOPO/TOP (132° cone angle), suggesting that the packing of alkyl chains would not be as sterically hindered as in the case of TOP/TOPO capped nanocrystals.[48] Furthermore, oleylamine has a C═C double bond. This rigid segment in the middle of the alkyl chain inhibits its backbending (known to occur in saturated C18 alkyl chains) and the large effective surface footprint that would derive from it.[49]

^{1}H and ^{13}C NMR data on colloidal dispersions of the Bi_2S_3 nanowires confirm binding of oleylamine based on the disappearance of the signals from the alpha and beta protons/carbons. T_2 relaxation times decrease upon binding of ligands to nanocrystals, which in part is responsible for the broadening of the peaks. The interaction of oleylamine with the various surface Bi atoms (i.e., two ligands vs one per Bi, accessible vs less accessible) also produces chemically and magnetically inequivalent environments, which leads to chemical shift distribution and further line broadening. This is consistent with our proposed model in which there are several distinct surface Bi atom sites.

Both XPS and NMR/UV−vis produced a N/Bi ratio of approximately 4.3. Since 75% of Bi atoms can be considered

(47) Seligson, A. L.; Trogler, W. C. *J. Am. Chem. Soc.* **1991**, *113*, 2520–2527.
(48) Tolman, C. A. *Chem. Rev.* **1977**, *77*, 313–348.
(49) Goodman, J. M. *J. Chem. Inf. Comput. Sci.* **1997**, *37* (5), 876–878.

to be on the surface, the ratio of $N/Bi_{surface}$ is 5.7. This provides enough oleylamine to allow for two oleylamine molecules to coordinate to the accessible Bi atoms and one to the less accessible Bi atoms. However, it also suggests that there are excess oleylamine molecules present in solution. The ^1H NMR spectrum from the purified nanowires shows no separate peaks for free and bound oleylamine (Figure 6b). This is the case even after adding additional oleylamine (Figure 6c,d). As mentioned previously, this establishes that the exchange between free and bound oleylamine is fast on the NMR time scale. The fast exchange results in the observation of a range of chemically and magnetically inequivalent environments, with ligands interacting with not only different surface Bi atoms but also other ligands during the exchange process. This further contributes to chemical shift distribution and line broadening, which is consistent with the broad NMR spectrum. This process could not be slowed down even at −60 °C, indicating that oleylamine can exchange and move between various surface Bi sites very easily. This also suggests that surface Bi atoms are not sterically crowded, as crowding would likely lead to a higher activation energy for exchange, which would be observed in the VT NMR. The ease of ligand exchange between oleylamine and hexadecylamine also is consistent with the low activation energy for exchange. Further study will be required to understand the complex exchange process, and work is underway to separate the different chemical environments of oleylamine using NMR diffusion spectroscopy.[16]

Conclusion

A model of the inorganic core and organic capping layer of ultrathin Bi_2S_3 nanowires has been constructed based on EXAFS, XANES, XPS, and NMR. This model includes a Bi_2S_3 core that closely resembles the bulk crystal structure (bismuthinite phase) with 75% of Bi atoms accessible to the ligands. The surface Bi atoms form Bi−N metal−ligand bonds with up to two oleylamine molecules depending on their accessibility. This coordination model is the only one that justifies the observed increased coordination number of bismuth determined by EXAFS along with solution phase NMR and solid state N 1s XPS. The value of the Bi coordination number proves that the nanowires possess an essentially complete capping when in the presence of an excess of oleylamine. The exchange between free and bound oleylamine occurs on time scales much faster than those accessible by NMR, even at low temperature. In addition to elucidating the core and surface structure of these ultrathin nanowires, we believe that these results demonstrate that the combination of solution phase XAS and NMR can be used successfully for the structural determination of nanostructures at the cluster to nanocrystals transition whose diameter is too small and their structure too beam sensitive to be effectively characterized with traditional techniques such as PXRD and HRTEM.

Acknowledgment. GAO is Government of Canada Research Chair in Materials Chemistry and Nanochemistry. We thank NSERC and the University of Toronto for generous and continued financial assistance, Ning Chen and Yongfeng Hu of the CLS for assistance with XAS and EXAFS measurements, Tim Burrow and Adina Golombek for assistance with VT NMR, and Peter Brodersen for assistance with XPS. The CLS is supported by NSERC, CIHR, NRC, and U. of Saskatchewan.

Supporting Information Available: Powder X-ray diffraction of Bi_2S_3 standard, additional NMR spectra, X-ray photoelectron spectra, and TEM images are available. This material is available free of charge via the Internet at http://pubs.acs.org.

JA101908K